Molecular Biology of the Cell
Vol. 14, 396–406, February 2003

Actin Filament Polymerization Regulates Gliding Motility by Apicomplexan Parasites[V]

D.M. Wetzel,* S. Håkansson,*‡ K. Hu,† D. Roos,† and L.D. Sibley*§

*Department of Molecular Microbiology, Washington University School of Medicine, St. Louis, Missouri 63110; †Department of Microbiology, University of Pennsylvania, Philadelphia, Pennsylvania 19104; and ‡Department of Molecular Biology, Umeå University, Umeå, Sweden 5-90187

Submitted August 2, 2002; Revised September 25, 2002; Accepted October 25, 2002
Monitoring Editor: Jennifer Lippincott-Schwartz

Host cell entry by *Toxoplasma gondii* depends critically on actin filaments in the parasite, yet paradoxically, its actin is almost exclusively monomeric. In contrast to the absence of stable filaments in conventional samples, rapid-freeze electron microscopy revealed that actin filaments were formed beneath the plasma membrane of gliding parasites. To investigate the role of actin filaments in motility, we treated parasites with the filament-stabilizing drug jasplakinolide (JAS) and monitored the distribution of actin in live and fixed cells using yellow fluorescent protein (YFP)-actin. JAS treatment caused YFP-actin to redistribute to the apical and posterior ends, where filaments formed a spiral pattern subtending the plasma membrane. Although previous studies have suggested that JAS induces rigor, videomicroscopy demonstrated that JAS treatment increased the rate of parasite gliding by approximately threefold, indicating that filaments are rate limiting for motility. However, JAS also frequently reversed the normal direction of motility, disrupting forward migration and cell entry. Consistent with this alteration, subcortical filaments in JAS-treated parasites occurred in tangled plaques as opposed to the straight, roughly parallel orientation observed in control cells. These studies reveal that precisely controlled polymerization of actin filaments imparts the correct timing, duration, and directionality of gliding motility in the Apicomplexa.

INTRODUCTION

Toxoplasma gondii, a pathogen of the immunocompromised and neonates, belongs to the phylum Apicomplexa. This group of parasites is unified by a highly structured apical complex that consists of secretory vesicles and cytoskeletal elements. Other members of this phylum include *Plasmodium spp*. (the causative agents of malaria) and *Cryptosporidium parvum* (an agent of waterborne diarrheal disease) as well as animal pathogens. Because apicomplexans are obligate intracellular parasites with complex life cycles, it is imperative that they be able to invade cells and migrate through tissues to be successful (Barragan and Sibley, 2002). Available evidence indicates that they accomplish these events by active motility, but the cellular basis of apicomplexan motility is poorly understood.

Cell invasion and tissue migration by apicomplexans are performed by a novel form of locomotion called gliding motility, which propels parasites across a substrate without the aid of cilia, flagella, or other locomotory organelles (Russell and Sinden, 1981; King, 1988). Apicomplexan motility occurs by gliding of the cresent-shaped parasite across the substrate, and this differs from the crawling motility of amoeba (Mitchison and Cramer, 1996). Apicomplexans are eukaryotic cells and do not express pili; hence, their motility differs from gliding in bacteria, which involves type IV pili (Wu and Kaiser, 1995). Examination of extracellular *T. gondii* by time-lapse videomicroscopy demonstrates that gliding motility consists of several stereotypical behaviors, as follows: 1) circular gliding, which occurs only in a counterclockwise direction; 2) upright twirling, which occurs only in a clockwise direction; and 3) helical gliding, which combines a clockwise flip with forward motility to move the crescent-shaped parasite forward across the substrate (Håkansson *et al.*, 1999). Cytochalasin D (CytD) blocks both parasite motility and host cell invasion, implying that these two processes require intact actin filaments (Dobrowolski and Sibley, 1996). Importantly, genetic studies using CytD-resistant *T. gondii* show conclusively that gliding motility and cell invasion require the actin cytoskeleton of the parasite and not that of the host cell (Dobrowolski and Sibley, 1996). Myosin may also participate in apicomplexan gliding

Article published online ahead of print. Mol. Biol. Cell 10.1091/mbc.E02–08–0458. Article and publication date are at www.molbiolcell.org/cgi/doi/10.1091/mbc.E02–08–0458.

[V] Online version of this article contains video material. Online version is available at www.molbiolcell.org .

§ Corresponding author. E-mail address: sibley@borcim.wustl.edu.

motility because drugs that inhibit myosins block gliding and invasion of host cells (Dobrowolski *et al.*, 1997a). A recent biochemical characterization of the *T. gondii* myosin presumed to be involved in these processes, TgMyoA, demonstrates that it is a fast-step, single-headed, plus-end–directed motor with kinetic and mechanical properties similar to those of the fast muscle myosins (Herm-Gotz *et al.*, 2002).

A model that combines these critical features of motility suggests that locomotion is driven by coupling the translocation of surface adhesins to an actin–myosin motor beneath the parasite plasma membrane (Sibley *et al.*, 1998; Ménard, 2001). However, despite the dependence of these processes on filamentous actin, demonstration of actin filaments in apicomplexans has been extremely difficult. Filaments are not apparent in nonmotile parasites examined by conventional electron microscopy (Shaw and Tilney, 1999), and biochemical studies indicate that the vast majority of actin (>97%) is found in the monomeric state in both *T. gondii* (Dobrowolski *et al.*, 1997) and *Plasmodium falciparum* (Pinder *et al.*, 1998). Therefore, although the actin cytoskeleton of these parasites is required for gliding motility and cell invasion, it is difficult to reconcile an apparent lack of actin filaments with their essential role in these processes.

The cyclopeptide jasplakinolide (JAS) is a membrane-permeable probe for examining actin dynamics in live cells. JAS induces actin polymerization by several mechanisms, as follows: 1) lowering the critical number of actin subunits necessary to drive polymerization, 2) releasing monomeric actin from sequestering proteins, and 3) binding to and stabilizing filaments (Bubb *et al.*, 1994, 2000). Previous studies using *T. gondii* demonstrated that JAS treatment induces actin polymerization at the anterior end of the parasite, which causes the formation of a prominent apical protrusion (Shaw and Tilney, 1999). Also, static end-point assays showed that JAS treatment inhibits gliding motility and cell invasion (Poupel and Tardieux, 1999; Shaw and Tilney, 1999). These results were obtained with high doses of JAS (1–2 μM) and suggested that actin polymerization induced a state of rigor. However, Shaw and Tilney also commented that JAS-treated parasites "moved more rapidly" in some cases (data not shown), which appears to conflict with this model (Shaw and Tilney, 1999). To resolve this discrepancy, using videomicroscopy, we used low doses of JAS to determine how actin polymerization affects parasite gliding in real time. Our results demonstrate that, although actin filaments are normally absent in *T. gondii,* their induction results in increased motile behaviors.

MATERIALS AND METHODS

Parasite Culture

T. gondii tachyzoites of the RH strain were maintained by serial 2-d passage in HFF cell monolayers as previously described (Morisaki *et al.*, 1995). RH-strain parasites expressing β-galactosidase (2F) were used in biochemical assays (Dobrowolski *et al.*, 1997). RH-strain parasites that expressed a fusion of the last 82 amino acid residues of TgMyoA with green fluorescent protein (GFP TgM-Atail) were provided by Dr. Dominique Soldati (Hettman *et al.*, 2000). Parasites were isolated soon after host cell lysis, passed through a 3-μm filter, and washed once with Hanks' balanced salt solution (Life Technologies, Gaithersburg, MD) containing 0.001 M EGTA, 0.01 M HEPES (HHE).

YFP-ACT1–Strain Construction

A plasmid expressing yellow fluorescent protein (YFP)-actin as a fusion protein was designed to have a 10-alanine linker between YFP and actin (Doyle and Botstei, 1996). The *ACT1* gene was amplified from a *T. gondii* cDNA plasmid by use of the PCR primers 5′-ACCAATGCAT*GCTGCCGCAGCGGCGGCAGCCGCTGCAGCA*-ATGGCGGATGAAGAAGTGCAAGC-3′ (ACT1F primer, containing coding sequence for 10 alanines [italicized]) and 5′-CATGCTTAATTAATTAGAAGCACTTGCGGTGGACG-3′ (ACT1R primer) and digested with *Nsi*I and *Pac*I. YFP was amplified by PCR using the primers 5′-ACGTCAGATCTAAAATGGTGAGCAAGGGCGAGG AGC-3′ (YFPF primer) and 5′-CAGTATGCATCTTGTACAGCTCGTCCATGCCG-3′ (YFPR primer) and digested with *Bgl*II and *Nsi*I. This construct, referred to as pTUB/YFP-ACT1/SAGCAT, contained the YFP-ACT1 fusion flanked by 5′-α-tubulin (Nagel and Boothroyd, 1988) and 3′-DHFR (Roos, 1993) regulatory sequences, followed by a chloramphenicol resistance cassette including the *CAT* gene flanked by *SAG1* regulatory sequences (Striepen *et al.*, 1998). Freshly isolated parasites ($n = 10^7$) were transfected with 75 μg plasmid DNA and inoculated into host cells as previously described (Roos *et al.*, 1994). To produce stable transgenics, chloramphenicol was added 24 h later to a final concentration of 6 μg/ml, and drug-resistant clones were isolated by limiting dilution after several rounds of selection. Transformants were further subcloned in the presence of drug; clone YA2 was selected for further use. Rabbit polyclonal anti-actin sera (Dobrowolski *et al.*, 1997) and mouse monoclonal antibody (mAb) 3E6 against GFP (Clontech, Cambridge, UK) were used to detect the YFP-actin protein in Western blots. Mouse mAb Tg17–43 against GRA1 (Cesbron-Delauw *et al.*, 1989) was used as a loading control.

Southern Blotting

Genomic DNAs from HFF cells or *T. gondii* (wild-type or YFP-ACT1 transgenics) were digested with restriction endonucleases at 37°C overnight, electrophoresed in 0.8% agarose gels, and transferred to nylon membranes by alkaline capillary transfer (Maniatis *et al.*, 1982). Blots were probed overnight with a ^{32}P-labeled probe encompassing a partial actin sequence of 241 nucleotides generated from the plasmid pTUB/YFP-ACT1/SAGCAT by PCR using the primers 5′-GACGACATGGAGAAAATCTGGCATCACACC-3′ (probeF primer)and 5′-CATGCTTAATTAATTAGAAGCACTTGCGGTGGACG-3′ (probeR primer). Blots were hybridized at 42°C overnight in 4× SSPE, 0.8% SDS, 40% formamide, 4× Denhardt's solution, and 100 μg/ml calf thymus DNA and washed at a final stringency of 68°C in 0.1× SSPE, 0.1% SDS. Filters were exposed to Kodak XAR film at −70°C for autoradiography.

Immunofluorescence Labeling

Parasites were resuspended in HHE and treated with 2 μM JAS (Molecular Probes, Eugene, OR) that had been dissolved in dimethylsulfoxide (DMSO) or 1% DMSO alone as a control for 10 min at room temperature, then allowed to adhere to poly-L-lysine–coated coverslips for 10 min in a hydrated chamber. Coverslips were rinsed, fixed for 5 min with 100% methanol at −20°C, and blocked with 20% FBS (Hyclone, Logan, UT) in PBS for 30 min. After labeling with rabbit polyclonal anti-ACT1 sera (Dobrowolski *et al.*, 1997) at 1:250 in PBS, rabbit anti-α-tubulin sera (Morrissette and Sibley, 2002b) at 1:1000, mouse monoclonal anti-SAG1 antibody (DG52) (Morisaki *et al.*, 1995) at 1:250, and/or mouse monoclonal anti-IMC1 (inner membrane complex) (45.15) antibody at 1:1000 in PBS (Mann and Beckers, 2001), parasites were labeled with goat anti-mouse or anti-rabbit Alexa 488 and/or 594 (1:500 in PBS, Molecular Probes). Samples were mounted in Vectashield + DAPI (Life Technologies) and examined with a Zeiss Axioskop or a Zeiss 510 confocal microscope (Zeiss, Oberkochen, Germany). Wide-field fluorescence images were collected with a Zeiss Axiocam and Zeiss Axiovision software version 2.0.5, then processed and merged with

Adobe Photoshop (Adobe Systems, Mountain View, CA). Confocal micrographs were taken with a 63× oil plan-apochromat objective lens (numerical aperture, 1.4; Zeiss) and He-Ne and Kr-Ar lasers. Images were imported into Zeiss Imagebrowser software and then processed in Adobe Photoshop.

Gliding Motility Assay

Coverslips were coated in 50% FBS in PBS for 1 h at 37°C and rinsed in PBS. Freshly harvested tachyzoites were resuspended in HHE, treated with varying concentrations of JAS or 1% DMSO for 10 min, added to precoated coverslips, and incubated at 37°C for 15 min. Slides were fixed in −20°C methanol and blocked with 20% FBS in PBS. The presence of the surface membrane protein SAG1 in trails was detected with mAb DG52 (1:250) conjugated directly to Oregon green (Molecular Probes). Coverslips were rinsed, mounted in Vectashield (Vector Laboratories, Burlingame, CA) plus DAPI, and examined with wide-field fluorescence microscopy. Average trail length in parasite body lengths (7 μm) was determined from five randomly selected 63× fields that contained ~50 parasites per field in each of three separate experiments (mean ± SEM).

Invasion Assay

HFF cells were plated on coverslips 24 h before experiments. Freshly harvested tachyzoites were resuspended in invasion media (DMEM, Life Technologies), 3% FBS, 10 mM HEPES) and used to challenge HFF monolayers for 15 min at 37°C. Monolayers were rinsed in HHE, fixed in 3% formaldehyde in PBS for 15 min at room temperature, blocked with 20% FBS in PBS, and stained with mAb DG52 (1:250) conjugated to Texas Red (Molecular Probes). Samples were then rinsed, permeabilized with 0.1% saponin for 15 min at room temperature, and stained with DG52 conjugated to Oregon green (1:250). Coverslips were rinsed, mounted in Vectashield, and examined with wide-field fluorescence microscopy. The percentage of intracellular parasites (green-stained but not red-stained) was determined from five randomly selected 63× fields that contained ~50 parasites per field in each of three separate experiments (mean ± SEM).

Quantification of Filamentous Actin by Western Blotting

Freshly harvested 2F-strain parasites (RH transfected with β-galactosidase) were placed in actin stabilization buffer (60 mM PIPES, 25 mM HEPES, 10 mM EDTA, 2 mM $MgCl_2$, 125 mM KCl) and treated with varying concentrations of JAS or 1% DMSO for 10 min at 37°C. Glycerol was added to a final concentration of 10%, 100× protease inhibitor cocktail (1 mg/ml E64, 10 mg/ml phenylmethylsulfonyl fluoride, 10 mg/ml TLCK (Nα-p-Tosyl-L-lysine-chloromethyl ketone hydrochloride), and 1 mg/ml leupeptin) was added to a final concentration of 1×, and Triton X-100 was added to a final concentration of 1%. Samples were incubated at 0°C for 1 h, then spun at 16,000 × *g* in an Eppendorf centrifuge 1415C at 4°C for 30 min to pellet actin filaments. The supernatant was mixed with an equal volume of acetone (Fisher Scientific, Houston, TX) and pelleted at 16,000 × *g* at 4°C for 20 min. These samples and parasite lysates (Dobrowolski and Sibley, 1996) were resuspended in protein gel sample buffer. Supernatants were loaded onto protein gels at 25% the concentration of the pellet samples. Actin was detected with a rabbit anti-ACT1 polyclonal antibody at 1:10,000 (Dobrowolski *et al.*, 1997). As a control for lysis, samples were blotted with a mouse monoclonal anti-β-galactosidase antibody (40–1a) at 1:30 (Dobrowolski *et al.*, 1997). Signals were enhanced with a horseradish peroxidase–conjugated secondary antibody to rabbit or mouse (1:10,000) and detected with the ECL+Plus Western blotting detection system (Amersham Biosciences, Piscataway, NJ). Western blots were quantified with a Molecular Dynamics (Sunnyvale, CA) Storm 860 phosphoimager and Bio-Rad (Hercules, CA) Molecular Analyst software.

Electron Microscopy

Parasites were resuspended in mammalian Ringer's solution (in mM: 155 NaCl, 3 KCl, 2 $CaCl_2$, 1 $MgCl_2$, 3 NaH_2PO_4, 10 HEPES, 10 glucose) at ~10^8 parasites per milliliter and pretreated with 2 μM JAS, 1% DMSO, or 1 μM CytD (Molecular Probes) for 10 min at room temperature before being allowed to glide on poly-L-lysine–coated coverslips for 10 min at 37°C. Coverslips were sonicated in KHMgE (in mM: 70 KCl, 30 HEPES, 5 $MgCl_2$, 3 EGTA at a pH of 7.2–7.4) plus 2 μM JAS, 1% DMSO, or 1 μM CytD with a microprobe mounted on a Mega-Mix Sonicator (GCA/Precision Scientific, Winchester, VA) for three pulses of ~5 s each at maximum intensity. Samples were then fixed in KHMgE plus 2% glutaraldehyde, rapidly frozen in liquid nitrogen, freeze-dried, and platinum-coated as described previously (Håkansson *et al.*, 1999). Replicas were examined and photographed with a JEOL CX100 transmission electron microscope (Jeol, Peabody, MA).

Videomicroscopy

Freshly isolated parasites were resuspended in Ringer's solution containing 1% FBS, treated with varying concentrations of JAS, 1 μM latrunculin B (LatB) (Molecular Probes), or 1% DMSO, and allowed to glide on glass-bottom microwells (MatTek Corp, Ashland, MA) precoated with 50% FBS in PBS. Videomicroscopy was conducted using a Zeiss Axiovert equipped with phase contrast and epifluorescence microscopy and a temperature-controlled stage (Medical Systems Corp., Greenvale, NY) to maintain 37°C incubation as described previously (Håkansson *et al.*, 1999). The optical path in this microscope is corrected to simulate an upright orientation, and thus objects appear in their true orientation with respect to the *x* and *y* planes. Motility was observed within minutes of addition of drug-treated parasites to the heated chamber and was recorded over a period of up to 30 min.

Images used for quantification were collected in real time under low-light illumination using an intensified CCD C2400 camera (Hamamatsu Photonics KK, Bridgewater, NJ) at 63× magnification. The video signal was digitally processed using a video-frame capture board (Perceptics Corp, Knoxville, TN) controlled by Biological Detection Systems image analysis software (BDS Image V 1.4.1, Oncor Imaging, Gaithersburg, MD) running on a Macintosh Quadra 900 computer (Apple Computers, Cupertino, CA). The analog output was recorded to S-VHS tape using a JVC model SR-S360U videocassette recorder. For analysis, parasite tracks were traced from the video monitor onto transparency sheets. Run lengths and start and stop frames for each movement were used to calculate velocities. The length of *T. gondii* (7 μm) provided a magnification standard. Five examples from three separate experiments were analyzed to obtain mean ± SEM values.

Time-lapse images used to construct Figure 4 and the supplemental videos were collected under low-light illumination with a Hamamatsu ORCA ER camera. Videos were recorded digitally at approximately eight frames per second with Openlab version 3.0.5 (Improvision, Lexington, MA), cropped, imported into Adobe Premiere 6.0, and saved as Quicktime movies.

RESULTS

Expression of YFP actin in T. gondii

To monitor actin dynamics in live cells, we tagged the single isoform of actin expressed by *T. gondii* with YFP (Striepen *et al.*, 1998). A transgenic strain of RH that expressed YFP fused to the N-terminus of *T. gondii* actin (ACT1) was constructed and subcloned, yielding YFP-ACT1 clone YA2 (Figure 1A). Wide-field fluorescence microscopy demonstrated that in

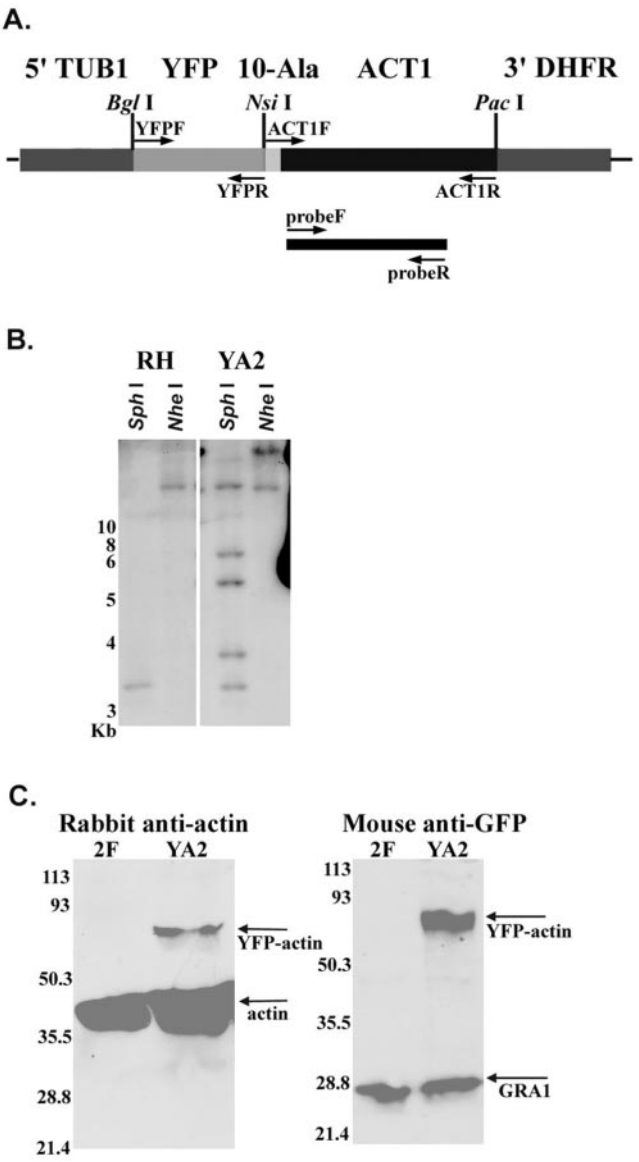

Figure 1. Expression of YFP actin in transgenic *T. gondii.* (A) Diagram of the YFP-actin construct (YFP-ACT1) used to transfect the RH strain of *T. gondii,* yielding strain YA2. A 10-alanine linker joins the YFP and actin (ACT-1) sequences. Expression of YFP-ACT1 is controlled by the tubulin promoter (5′-TUB1) and the 3′-DHFR sequence. Restriction sites used during construction of YFP-ACT1 are indicated above the diagram. PCR primers are indicated by arrows. The probe used in B is illustrated by the black bar. (B) Southern blot illustrating the copy number of YFP-ACT1 in YA2. Left, RH-strain (wild-type) genomic DNA digested with *Sph*I and *Nhe*I and probed with a partial actin sequence. Right, YA2 genomic DNA visualized with the same probe after digestion with the same restriction enzymes. (C) Western blot demonstrates that YFP-ACT1 is expressed in strain YA2 but not in 2F (RH transfected with β-galactosidase). Left, probed with anti-ACT1 polyclonal sera. Right, probed with monoclonal anti-GFP antibody 3E6. Mouse mAb Tg17–43 against an unrelated protein, GRA1, was used as a loading control. Numbers refer to molecular mass in kDa.

this clone, YFP-ACT1 had the same distribution as actin detected with polyclonal anti-actin sera (data not shown). Southern blot analysis of this strain revealed patterns consistent with multiple insertions (approximately four copies) of YFP-ACT1 into the genome of YA2 (Figure 1B). In addition, the wild-type copy of actin remained unaltered. Despite the multiple insertions of YFP-ACT1, Western blot analysis of whole-cell extracts of YA2 using rabbit polyclonal anti-actin sera demonstrated that YFP-ACT1 was expressed at levels substantially below those of wild-type actin (Figure 1C). The level of wild-type actin was not significantly changed in YFP-ACT1–expressing parasites, despite the modest increase seen in Figure 1C (data not shown). A mouse mAb to GFP reacted with full-length YFP-ACT1 in YA2 and did not react to 2F parasites (RH-strain parasites expressing β-galactosidase) (Figure 1C). Antibodies to the dense-granule protein GRA1 were used as a loading control (Figure 1C).

JAS Alters the Distribution of Actin But Not Other Cytoskeletal Elements in T. gondii

Previous studies demonstrated that treatment of *T. gondii* with high doses (1–2 μM) of JAS induces actin polymerization in the parasite, which leads to a prominent apical protrusion of actin filaments (Shaw and Tilney, 1999). However, the effects of JAS treatment on other cytoskeletal elements have not been investigated. Therefore, we examined the effects of JAS on the distribution of actin and the other major cytoskeletal elements in the parasite, which include microtubules, reticular filaments found beneath the inner membrane complex (IMC) (represented by IMC-1), and the small myosin TgMyoA, which has been implicated in gliding motility (Hettman *et al.*, 2000; Morrissette and Sibley, 2002).

Treatment with JAS induced profound changes in the normally diffuse pattern of YFP-ACT1 fluorescence in YA2, resulting in a marked polarity of staining at the apical and posterior ends of the cell, as indicated by epifluorescence microscopy (Figure 2A). The apical extension of actin filaments was similar to that previously reported by electron microscopy (EM) (Shaw and Tilney, 1999); however, YFP-ACT1 was also strongly localized at the posterior end, a result that was enhanced by staining with antibodies to *T. gondii* ACT1. Time-lapse videomicroscopy of YA2 parasites demonstrated that actin relocalization occurred within minutes of drug addition (data not shown). Confocal microscopy was used to further examine the actin localized at the posterior end of wild-type parasites. Staining with an antibody to actin demonstrated that actin relocalized by JAS treatment formed a posterior spiral. This spiral appeared to be located directly beneath the plasma membrane, because the integral membrane protein SAG1 was observed in the same focal plane as actin (Z-step = 0.4 μm) (Figure 2B).

In stark contrast to the redistribution of actin that was induced by JAS, no changes in the distribution of microtubules or IMC-1 were apparent in JAS-treated cells (Figure 2A). TgMyoA was located at the membrane in all control and JAS-treated parasites, and it accumulated at the apical end of ~50% of both control and JAS-treated cells. Notably, TgMyoA did not follow actin into the apical extensions that formed with JAS treatment (Figure 2A). In addition, no changes were noted in the distribution of two actin-binding proteins known in *T. gondii*: toxofilin (a monomer sequestering protein) (Poupel *et al.*, 2000) and

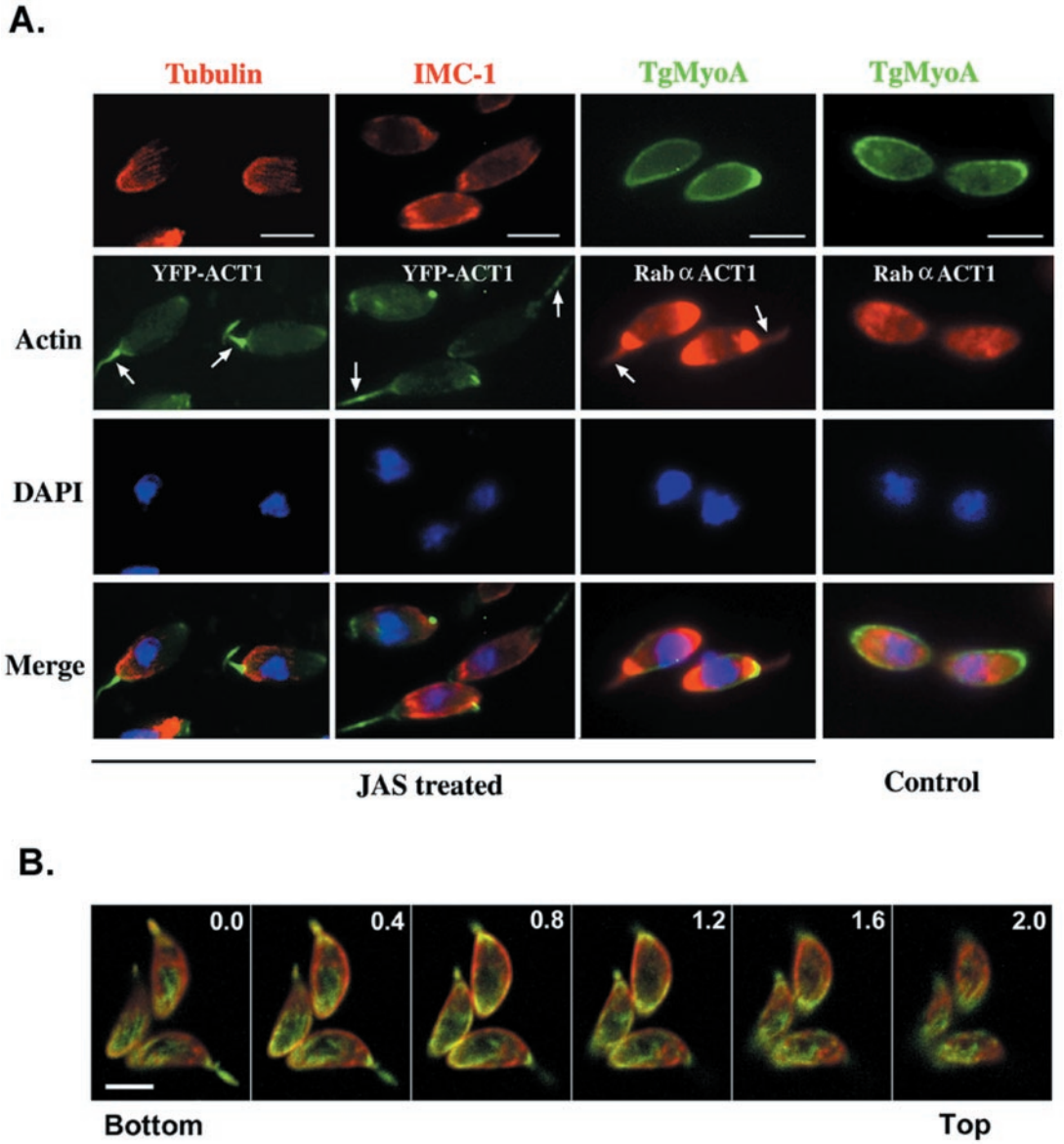

Figure 2. Distribution of cytoskeletal elements in JAS-treated *T. gondii*. (A) Wide-field fluorescence microscopy demonstrates that JAS alters the distribution of actin in *T. gondii* but does not affect microtubules (tubulin), reticular network filaments (IMC1), or myosin (TgMyoA tail). Arrows indicate the apical extensions of actin that form with JAS treatment. Strongly staining posterior localization of actin is also seen in JAS-treated but not control cells. Bar, 5 μm. (B) Confocal microscopy shows the posterior actin spiral that is induced beneath the parasite plasma membrane by JAS treatment. SAG1 (red) was visualized with mAb DG52, followed by goat anti-mouse Alexa 594. Actin (green) was visualized by staining of rabbit polyclonal anti-ACT1 followed by goat anti-rabbit Alexa 488. Each panel represents a 0.4-μm section starting from the edge of the parasite attached to the bottom coverslip. Pinhole, 0.4 μm. Bar, 5 μm.

an actin-depolymerizing factor (ADF)/cofilin homolog (Allen *et al.*, 1997) (data not shown). These results indicate that the sole influence of JAS on the cytoskeleton of the parasite is redistribution of actin.

JAS Treatment of T. gondii *Induces Actin Polymerization*

To determine the dose-dependent effects of JAS on actin polymerization, we analyzed the distribution of actin in detergent extracts by quantitative Western blotting. In untreated parasites, only a small fraction (~3%) of actin was present in the detergent-insoluble fraction, representing polymerized or F-actin (Figure 3, A and B). JAS treatment induced a dose-dependent increase in detergent-insoluble actin (pelleted at 16,000 $\times$ *g*), which reached a maximum of >25% of total actin. Centrifugation of samples at 100,000 $\times$ *g* did not increase the amount of actin pelleted in controls or JAS-treated samples (data not shown). Interestingly, *T. gon-*

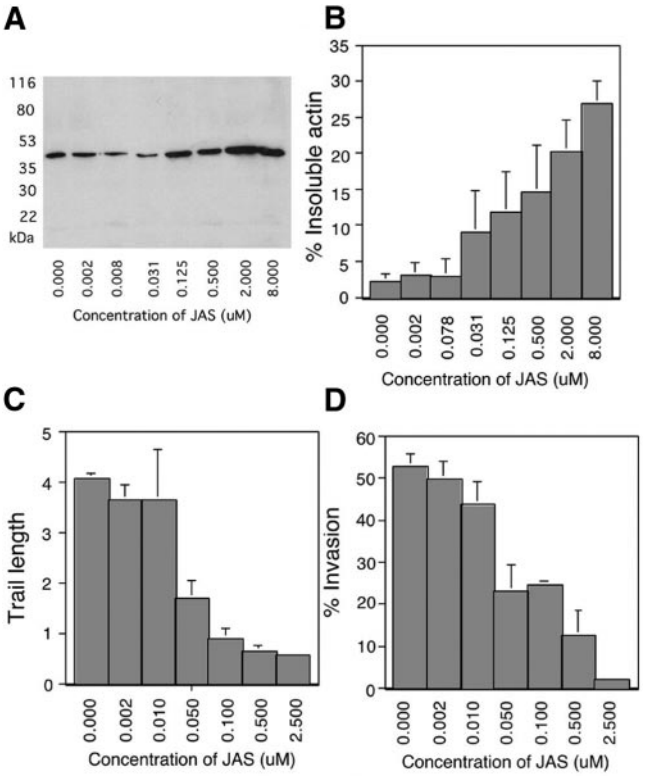

Figure 3. Effects of JAS treatment on *T. gondii* actin polymerization, trail formation, and invasion. In control parasites, the vast majority of actin was detergent-soluble (monomeric), and the amount of F-actin increased proportionally with JAS treatment. (A) Western blot analysis of the filamentous actin in 2F (RH-strain parasites expressing β-galactosidase). Parasites were treated with JAS or DMSO and lysed with detergent, then filamentous actin was pelleted by centrifugation. Equal cell equivalents of insoluble fractions (F-actin) were loaded in each lane; all lanes were probed with anti-actin antibody. (B) Phosphoimager quantification of Western blots demonstrated that the percentage of F-actin increased with increasing concentrations of JAS. Values were normalized for cell lysis as determined by release of β-galactosidase from the cytosol. Bars represent the average of four separate experiments (mean ± SEM). (C) The average length of the trails deposited during gliding decreased with increasing concentrations of JAS. Parasites were treated with JAS or DMSO and allowed to glide on serum-coated glass. Trails were visualized with anti-SAG1 antibody. Bars show average trail length in parasite body lengths (7 μm) from five randomly selected fields that contained ~50 parasites per field in each of three separate experiments (mean ± SEM). (D) Percentage of parasites invading host cells decreased with increasing concentrations of JAS. Parasites were treated with JAS or DMSO and allowed to invade HFF cells. A two-color immunofluorescence assay was used to distinguish between intracellular and extracellular parasites. Bars show the average percentage of intracellular parasites (green but not red) from five randomly selected high-power microscope fields that contained ~50 parasites per field from three separate experiments (mean ± SEM).

dii was extremely sensitive to the effects of JAS. Parasite actin polymerization was first detected after treatment with drug concentrations between 0.031 and 0.125 μM, much lower doses than those previously used to assay the effects of actin filament stabilization in *T. gondii* (Poupel and Tardieux, 1999; Shaw and Tilney, 1999) or in other systems (Bubb *et al.*, 1994, 2000).

JAS Treatment of T. gondii *Blocks Trail Formation and Cell Invasion*

Previous studies indicate that high doses of JAS (1–2 μM) inhibit trail formation (Poupel and Tardieux, 1999) and cell invasion (Poupel and Tardieux, 1999; Shaw and Tilney, 1999) by *T. gondii*. We examined the dose-dependent effects of JAS on migration and cell entry to determine whether inhibition of these processes corresponded to the effects of JAS on filament formation. Migration across the substrate was decreased in a dose-dependent manner by JAS treatment, as demonstrated by reduced trail formation by gliding parasites (Figure 3C). JAS also inhibited invasion of parasites into host cells in a dose-dependent manner (Figure 3D). Again, *T. gondii* was exquisitely sensitive to JAS, since disruption of these processes occurred at 20-fold lower concentrations of drug than previously examined (Poupel and Tardieux, 1999; Shaw and Tilney, 1999). Inhibition of gliding and invasion was half-maximal at a concentration of 0.05 μM, similar to the dose at which actin polymerization was first detected (Figure 3, A and B). The effects of JAS on filament polymerization, gliding, and cell invasion were fully reversible after a 10-min treatment and 5-min washout (data not shown). These results indicate that the effects of JAS are transient and suggest they are limited to the induction of actin polymerization. This conclusion differs from a previous report that observed no reversal in these phenotypes when the level of JAS was reduced by dilution (Poupel and Tardieux, 1999). However, as we show here, such reduced levels of JAS still have profound activity on the parasite.

JAS Treatment Increases the Speed of T. gondii *Gliding Motility and Causes Frequent Direction Reversals*

The inhibition of trail formation and invasion by JAS suggests that actin polymerization induces a state of rigor in the parasite, similar to the effects of actin depolymerization by CytD, as reported (Dobrowolski and Sibley, 1996; Håkansson *et al.* 1999). However, other authors previously commented that JAS treatment makes *T. gondii* more active, although no data were provided on specific changes in motility (Shaw and Tilney, 1999). To address this discrepancy, as well as to examine the effects of actin polymerization on parasite motility in real time, we monitored parasite gliding by videomicroscopy.

When viewed from the front of the cell, control parasites invariably twirl their anterior end in a clockwise direction (Figure 4A; Video 1). Surprisingly, JAS treatment increased the speed of twirling approximately threefold and often reversed the direction of twirling from clockwise to counterclockwise (Figure 4B; Table 1; Videos 2 and 3). The normal circular gliding behavior of control *T. gondii* was not observed in JAS-treated parasites, indicating that it was disrupted by the alterations in actin that occur with treatment (Table 1). In addition, JAS treatment had profound effects on helical gliding. Helical gliding in

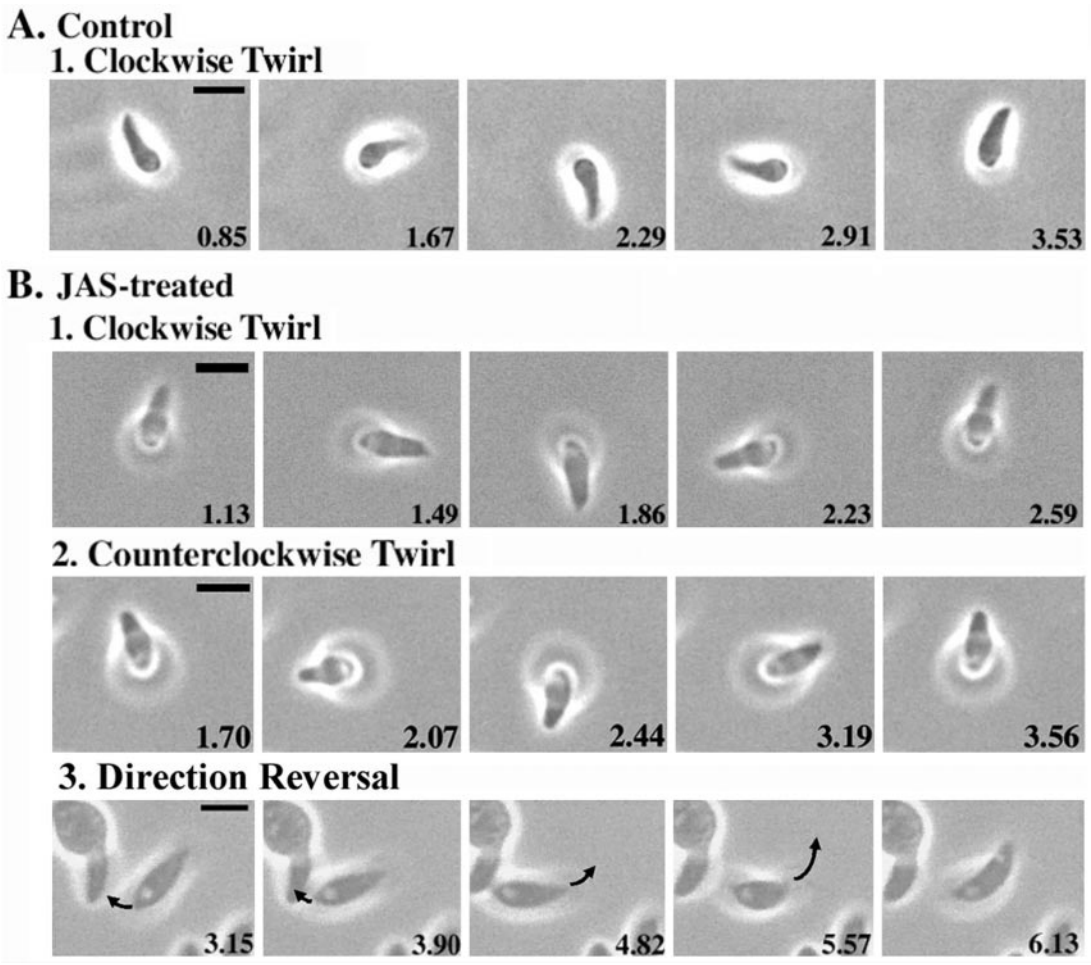

Figure 4. Videomicroscopy analysis of gliding motility in JAS-treated *T. gondii*. JAS treatment increased the gliding speed of parasites and caused frequent reversal of direction. Extracellular parasites were treated with 2 μm JAS or DMSO, allowed to glide, and recorded with time-lapse videomicroscopy. Each panel shows a single still frame taken from the supplemental videos. Elapsed time is indicated in seconds in the lower right of each frame. Bar, 5 μm. (A) Upright twirling in control gliding *T. gondii* always occurs in a clockwise direction. Example is from Video 1. (B) JAS treatment increased the speed of normal clockwise twirling (1) and often caused direction reversal, resulting in counterclockwise spirals (2). Example in B1 is taken from Video 2, example in B2 is taken from Video 3. JAS treatment also led to frequent direction reversals in gliding parasites (3). In the example shown (from Video 4), the parasite in the center first moves toward the left and then reverses direction, moving upward and to the right. Polarity is indicated by a prominent vacuole; arrow illustrates direction of movement between successive frames.

control cells always proceeds in a forward direction, with the apical end of the parasite leading. During this forward movement, the arc-shaped parasite glides along its convex surface, tracing out a spiral pattern as it moves forward (consult the videos published in Håkansson *et al.*, 1999). JAS-treated parasites began moving forward but then rapidly reversed or altered direction (Figure 4B; Video 4). This frequent reversal of direction often resulted in a behavior called "rolling," during which the parasite moved forward, raising its anterior end off the substrate, then reversed course, elevating the posterior end (Video 5). The rate of movement during rolling was considerably faster than normal helical gliding motility (Table 1). However, despite their high degree of motility, rolling parasites were unable to make any forward progress across the substrate. In contrast to the enhancement of gliding demonstrated with JAS treatment, the actin-depolymerizing agent LatB prevented all forms of motility (Table 1). In addition, the myosin inhibitor 2,3-butanedione 2-monoxime (BDM) blocked JAS-induced motility without affecting filament stability (data not shown).

The duration of twirling in the presence of JAS often lasted up to 30 min, similar to that of control cells (data not shown), indicating that actin polymerization did not induce a state of rigor. In addition, the total percentage of parasites that underwent gliding motility was not altered by JAS treatment (typically, 5–10% were active during a 1-min sampling period). However, because of frequent changes in direction, JAS treatment reduced the average duration of a single uninterrupted segment of forward motion by almost

Table 1. Rates of gliding motility by *T. gondii*

	Control		JAS		LatB
Behavior	Occurrence	Rate[a]	Occurrence	Rate[a]	Occurrence
Twirl CW	+	0.37 ± 0.08 rev/s	+	0.98 ± 0.36 rev/s	−
Twirl CCW	−	NA	+	0.88 ± 0.37 rev/s	−
Circular	+	0.98 ± 0.19 μm/s	−	NA	−
Helical	+	1.64 ± 0.12 μm/s	−	NA	−
Roll	−	NA	+	5.51 ± 0.67 μm/s	−

[a] Mean ± SEM. CW, clockwise; CCW, counterclockwise; NA, not applicable.

10-fold. Sequences of sustained helical gliding in control, untreated *T. gondii* had an average duration of 29.575 ± 4.140 s. In contrast, JAS-treated parasites had a much shorter duration of sustained gliding of 3.172 ± 0.314 s (mean ± SEM, measured from 10 examples from three separate experiments).

Collectively, our findings revealed that JAS treatment increased the content of F-actin in *T. gondii*, and surprisingly, stabilizing filaments activated several motile behaviors in the parasite. However, because of frequent direction changes, this hyperkinetic behavior was actually counterproductive, effectively blocking migration across the substrate (as monitored by trail formation) and preventing cell invasion.

Actin-Like Filaments Are Formed in Gliding Parasites

The profound effects of JAS treatment on actin dynamics and motility suggested that initiation of new filaments is responsible for gliding motility. It has been hypothesized previously that the actin filaments that participate in gliding motility are located beneath the plasma membrane of the parasite (Sibley *et al.*, 1998; Ménard, 2001). Therefore, we examined the interior surface of the parasite cell membrane by sonicating gliding parasites to remove them from the substrate. Sonicated parasites left behind a plasma membrane footprint attached to the coverslip (Figure 5). The inner surface of control membrane footprints was decorated by longitudinal microfilaments extending from 0.2 to > 1 μm in length (Figure 5, A and B). These microfilaments exhibited several characteristic features of actin filaments, including 7- to 8-nm diameter and sensitivity to disruption by CytD (Figure 5E). On the basis of these features, we conclude that actin filaments form beneath the parasite plasma membrane during normal gliding.

Filaments deposited on parasite membrane footprints after JAS treatment demonstrated a different morphology than control filaments (Figure 5, C and D). Instead of parallel filaments, JAS-treated cells formed densely bundled mats of filaments that were randomly oriented. Filament arrays on the inner surface of host cell membranes displayed a typical intertwined branched pattern (Figure 5F).

DISCUSSION

Our studies help to resolve the apparent discrepancy that although actin filaments are needed for parasite motility, the vast majority of actin in apicomplexans is not normally polymerized. Using the compound JAS, we demonstrated that induction of actin polymerization has profound effects on parasite motility. Videomicroscopy showed that JAS increases the velocity of parasite motility but often disrupts directed gliding by causing frequent direction reversals. EM illustrated that actin filaments form beneath the parasite membrane during normal gliding, but randomly oriented actin filaments are induced by JAS treatment. Collectively, these effects lead to inhibition of directed gliding and invasion at drug concentrations that closely correspond to the dose at which actin polymerization is first detected in *T. gondii*. We conclude from these studies that manipulation of the polymerization state of actin imparts control of the initiation, duration, and direction of gliding motility in the Apicomplexa.

JAS treatment induces actin polymerization at the apical end of *T. gondii*, as previously visualized by EM (Shaw and Tilney, 1999). These authors suggested that the resulting apical projection may act like a jackhammer to drive cell invasion (Shaw and Tilney, 1999). However, the apical projection extends beyond the conoid, which normally extrudes during cell invasion (Mondragon and Frixione, 1996). Therefore, the formation of the apical projection is not likely to reflect the natural process of cell invasion. Filamentous actin may instead extend from the cell here, because only one membrane surrounds the parasite at its apical end, whereas three membranes enclose the remainder of the parasite (Morrissette and Sibley, 2002).

Not recognized previously, JAS treatment also results in the formation of filamentous actin spirals directly beneath the plasma membrane. These spirals could establish a scaffold for a myosin motor during twirling and helical gliding. Because BDM prevents both control and JAS-induced motility, it is likely that gliding motility in *T. gondii* depends on a myosin motor and is not simply driven by actin polymerization. Interestingly, TgMyoA, the myosin implicated in gliding in *T. gondii*, slides along purified actin filaments at ~5.2 μm/s (Herm-Gotz *et al.*, 2002), consistent with the maximum rate of gliding reported here after JAS treatment. Consequently, unlike in conventional systems, in which movement is controlled by changing the activation state of myosin, the polymerization of new actin filaments in *T. gondii* appears to regulate motility.

The IC_{50} of JAS determined here is much lower than that used in previous studies on *T. gondii* (Poupel and Tardieux, 1999; Shaw and Tilney, 1999). Filament formation induced

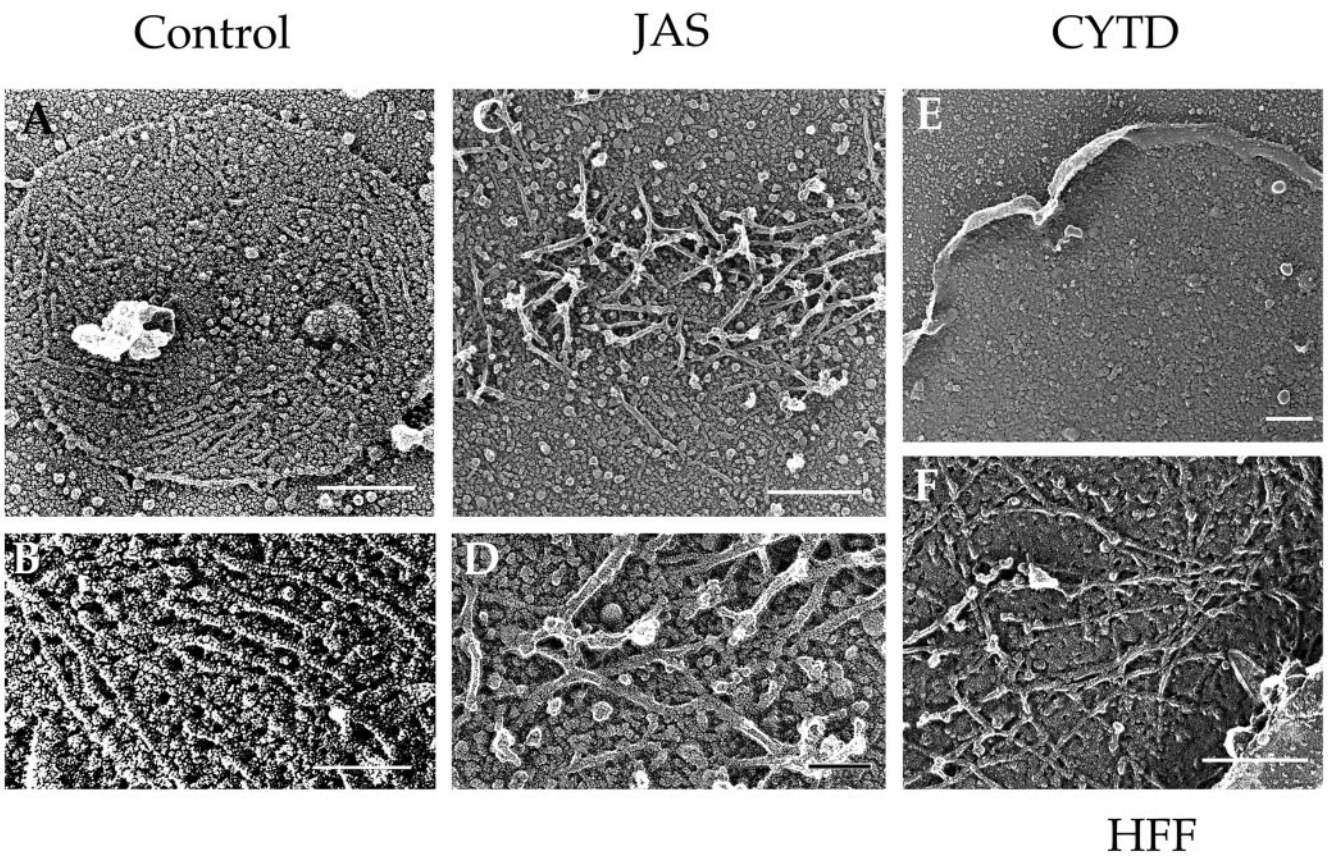

Figure 5. Freeze-dried platinum replicas of actin-like filaments in gliding *T. gondii*. Parasites were allowed to glide on coverslips, sonicated, and prepared for platinum-replica EM (Håkansson *et al.*, 1999). After sonication, the surface membrane of the gliding parasite remained attached to the substrate. The surface of the membrane that was originally exposed to the cytosol was decorated by filaments ranging from 0.2 to >1 μm in length. (A and B) In control parasites, short unbranched filaments were found on the cytoplasmic face of plasma membrane patches. (C) After treatment with JAS, parasite filaments were clustered in dense interwoven mats. (D) Parasite filaments formed in JAS were bundled in dense mats (enlarged from C). (E) Parasite filaments were disrupted in the presence of CytD, leaving only the bare membrane. (F) In control HFF cells, actin filaments under the membrane formed branched arrays. Bars in A, C, E, and F, 0.25 μm; in B and D, 0.1 μm.

by JAS treatment correlates with inhibition of trail formation and cell invasion, which suggests that these behavioral changes are induced solely by the formation of filamentous actin. This conclusion is further substantiated by immunofluorescence data that show that JAS has no obvious effects on other cytoskeletal elements.

Although static assays suggest that JAS prevents motility of *T. gondii*, video analyses reveal that dramatic alterations in parasite behavior occur with JAS treatment. In contrast, agents that depolymerize actin, such as LatB and CytD (Håkansson *et al.*, 1999), block all forms of motility. Thus, opposing effects on the polymerization state of actin in *T. gondii* result in opposite effects on parasite gliding motility. The speed of parasite gliding increases with JAS treatment, indicating that filament formation is the rate-limiting step for gliding motility. This hypothesis is strengthened by the visualization of parallel actin-like filaments beneath the membrane of motile but not static parasites. Unfortunately, the polarity of these filaments cannot be ascertained, because the sonication step in our EM preparations removes the parasite, preventing determination of its orientation. Surprisingly, JAS-treated parasites are able to glide both forward and backward, whereas control parasites are able to proceed only forward. This inability to undergo directed motion explains the lack of trail deposition demonstrated earlier (Poupel *et al.*, 2000) and in the present study. Consistent with this discovery, our EM data demonstrate that whereas filaments in control parasites are aligned, filaments that form after JAS treatment of gliding parasites are randomly oriented. These two results indicate that the direction of parasite gliding is probably controlled by the orientation of filaments that form beneath the plasma membrane.

Our data further establish that the regulation of actin dynamics in the Apicomplexa is fundamentally different from that in other organisms (Mitchison and Cramer, 1996). First, unlike most cells, which contain ~50% filamentous actin, the vast majority of actin in apicomplexan parasites is monomeric (Dobrowolski *et al.*, 1997). Second, a complex network of regulatory proteins drives actin-based motility in amoeba and vertebrate cells. In contrast, the only actin-regulatory proteins described in *T. gondii* to date are an actin-sequestering protein called toxofilin (Poupel *et al.*,

2000) and an ADF/cofilin homologue (Allen *et al.*, 1997), which is probably involved in filament severing. Presumably, these proteins, and possibly other regulatory mechanisms, serve to maintain the majority of actin in a monomeric state in apicomplexans. Third, in other organisms, motility requires both monomeric and filamentous actin, because both actin-stabilizing and actin-depolymerizing agents decrease movement (Mitchison and Cramer, 1996). In *T. gondii,* although actin-depolymerizing drugs block motility, JAS treatment (even at low concentrations) induces actin polymerization that drives hypermotile behavior.

Gliding motility in the Apicomplexa is clearly highly regulated. Resting, intracellular parasites are nonmotile. However, during tissue migration or after host cell lysis, these obligate intracellular parasites must rapidly invade a new host cell to survive, and once cell entry is complete, forward motility ceases. This transition from motile to sessile behavior occurs throughout the life cycle of not only *T. gondii* but also all other apicomplexans. For example, during its life cycle, *Plasmodium spp*. must travel from the mosquito midgut to the salivary glands. Then, after injection into the skin of a human host, *Plasmodium spp*. must make its way from the periphery to the liver, where it first develops, before it enters the circulation and ultimately invades red blood cells. Because gliding motility in other apicomplexans is highly similar to that described here for *T. gondii* (Russell and Sinden, 1981; Stewart and Vanderberg, 1988; Arrowwood *et al.*, 1991), it is likely that a common mechanism governs gliding motility in this important phylum of intracellular parasites.

The prevailing model of apicomplexan gliding motility predicts that locomotion is driven by coupling translocation of surface adhesins to an actin–myosin motor beneath the parasite plasma membrane (Sibley *et al.*, 1998; Ménard, 2001). We conclude from these studies that in resting parasites, the majority of actin is kept in the monomeric state and the gliding motility required to drive cell invasion or tissue migration is induced by the polymerization of oriented actin filaments. Our model makes the following predictions. First, polymerization of actin filaments must occur directly beneath the plasma membrane to facilitate translocation of cell-surface adhesins. Second, the polarity of actin filaments must be ordered to drive directional gliding. Finally, filament turnover must be tightly controlled to regulate the timing of motility. The speed of these processes suggests that filaments must be turned over rapidly. Unraveling the mechanisms of actin filament dynamics in the Apicomplexa will provide fundamental insight into the motility of these unusual organisms as well as highlight key differences in the biology of these parasites that may be exploited to prevent infection.

ACKNOWLEDGMENTS

We thank John Cooper, Daniel Goldberg, Dorothy Schaffer, and Wandy Beatty for helpful comments and critical review of this manuscript; Gary Ward (University of Vermont) for antibodies to IMC-1; Dominique Soldati (Imperial College of London) for the TgMyoA-GFP–expressing parasites; Naomi Morrissette for assistance with microscopy; and Robyn Roth and John Heuser for performing the freeze-fracture EM. Supported by the National Institutes of Health (NIH) (AI34036) (L.D.S.), the Burroughs Wellcome Fund (L.D.S.), NIH Institutional Training Grants AI017172–19 and T32 GM07200 (D.M.W.), and the Swedish Research Council (S.H.).

REFERENCES

Allen, L.H., Dobrowolski, J.M., Muller, H., Sibley, L.D., and Mansour, T.E. (1997). Cloning and characterization of actin depolymerizing factor from *Toxoplasma gondii*. Mol. Biochem. Parasitol. *88*, 43–52.

Arrowood, M.J., Sterling, C.R., and Healey, M.C. (1991). Immunofluorescent microscopical visualization of trails left by gliding *Cryptosporidium parvum* sporozoites. J. Parasitol *77*, 315–317.

Barragan, A., and Sibley, L.D. (2002). Transepithelial migration of *Toxoplasma gondii* is linked to parasite motility and virulence. J. Exp. Med. *195*, 1625–1633.

Bubb, M.R., Senderowicz, A.M.J., Sausville, E.A., Duncan, K.L.K., and Korn, E.D. (1994). Jasplakinolide, a cytotoxic natural product, induces actin polymerization and completely inhibits the binding of phalloidin to F-actin. J. Biol. Chem. *269*, 14869–14871.

Bubb, M.R., Spector, I., Beyer, B.B., and Fosen, K.M. (2000). Effects of jasplakinolide on the kinetics of actin polymerization. J. Biol. Chem. *275*, 5163–5170.

Cesbron-Delauw, M.F., Guy, B., Pierce, R.J., Lenzen, G., Cesbron, J.Y., Charif, H., Lepage, P., Darcy, F., Lecocq, J.P., and Capron, A. (1989). Molecular characterization of a 23-kilodalton major antigen secreted by *Toxoplasma gondii*. Proc. Natl. Acad. Sci. USA *86*, 7537–7541.

Dobrowolski, J.M., Carruthers, V.B., and Sibley, L.D. (1997a). Participation of myosin in gliding motility and host cell invasion by *Toxoplasma gondii*. Mol. Microbiol. *26*, 163–173.

Dobrowolski, J.M., Niesman, I.R., and Sibley, L.D. (1997b). Actin in *Toxoplasma gondii* is encoded by a single-copy gene, *ACT1*, and exists primarily in a globular form. Cell Motil. Cytoskeleton *37*, 253–262.

Dobrowolski, J.M., and Sibley, L.D. (1996). *Toxoplasma* invasion of mammalian cells is powered by the actin cytoskeleton of the parasite. Cell *84*, 933–939.

Doyle, T., and Botstei, D. (1996). Movement of yeast cortical actin cytoskeleton visualized in vivo. Proc. Natl. Acad. Sci. USA *93*, 3886–3891.

Håkansson, S., Morisaki, H., Heuser, J.E., and Sibley, L.D. (1999). Time-lapse video microscopy of gliding motility in *Toxoplasma gondii* reveals a novel, biphasic mechanism of cell locomotion. Mol. Biol. Cell *10,* 3539–3547.

Herm-Gotz, A., Weiss, S., Stratmann, R., Fujita-Becker, S., Ruff, C., Meyhofer, E., Soldati, T., Manstein, D.J., Geeves, M.A., and Soldati, D. (2002). *Toxoplasma gondii* myosin A and its light chain: a fast, single-headed, plus-end-directed motor. EMBO J. *21*, 2149–2158.

Hettman, C., Herm, A., Geiter, A., Frank, B., Schwarz, E., Soldati, T., and Soldati, D. (2000). A dibasic motif in the tail of a class XIV apicomplexan myosin is an essential determinant of plasma membrane localization. Mol. Biol. Cell *11*, 1385–1400.

King, C.A. (1988). Cell motility of sporozoan protozoa. Parasitol. Today *11*, 315–318.

Maniatis, T., Fritsch, E.F., and Sambrook, J. (1982). Molecular Cloning: A Laboratory Manual. Cold Spring Harbor, New York: Cold Spring Harbor Laboratory.

Mann, T., and Beckers, C. (2001). Characterization of the subpellicular network, a filamentous membrane skeletal component in the parasite *Toxoplasma gondii*. Mol. Biochem. Parasitol. *115,* 257–268.

Ménard, R. (2001). Gliding motility and cell invasion by Apicomplexa: insights from the Plasmodium sporozoite. Cell. Microsc. *3*, 63–73.

Mitchison, T.J., and Cramer, L.P. (1996). Actin-based cell motility and cell locomotion. Cell *84*, 371–379.

Mondragon, R., and Frixione, E. (1996). Ca^{2+}-dependence of conoid extrusion in *Toxoplasma gondii* tachyzoites. J. Eukaryot. Microbiol. *43*, 120–127.

Morisaki, J.H., Heuser, J.E., and Sibley, L.D. (1995). Invasion of *Toxoplasma gondii* occurs by active penetration of the host cell. J. Cell Sci. *108*, 2457–2464.

Morrissette, N.S., and Sibley, L.D. (2002a). Cytoskeleton of apicomplexan parasites. Microbiol. Mol. Biol. Rev. *66*, 21–38.

Morrissette, N.S., and Sibley, L.D. (2002b). Disruption of microtubules uncouples budding and nuclear division in *Toxoplasma gondii*. J. Cell Sci. *115*, 1017–1025.

Nagel, S.D., and Boothroyd, J.C. (1988). The alpha- and beta-tubulins of *Toxoplasma gondii* are encoded by single copy genes containing multiple introns. Mol. Biochem. Parasitol. *29*, 261–273.

Pinder, J.C., Fowler, R.E., Dluzewski, A.R., Bannister, L.H., Lavin, F.M., Mitchell, G.H., Wilson, R.J.M., and Gratzer, W.B. (1998). Actomyosin motor in the merozoite of the malaria parasite, *Plasmodium falciparum*: implications for red cell invasion. J. Cell Sci. *111*, 1831–1839.

Poupel, O., Boleti, H., Axisa, S., Couture-Tosi, E., and Tardieux, I. (2000). Toxofilin, a novel actin-binding protein from *Toxoplasma gondii*, sequesters actin monomers and caps actin filaments. Mol. Biol. Cell *11*, 355–368.

Poupel, O., and Tardieux, I. (1999). *Toxoplasma gondii* motility and host cell invasiveness are drastically impaired by jasplakinolide, a cyclic peptide stabilizing F-actin. Microbes Infect. *1*, 653–662.

Roos, D.S. (1993). Primary structure of the dihydrofolate reductase-thymidylate synthase gene from *Toxoplasma gondii*. J. Biol. Chem. *268*, 6269–6280.

Roos, D.S., Donald, R.G.K., Morrissette, N.S., and Moulton, A.L. (1994). Molecular tools for genetic dissection of the protozoan parasite *Toxoplasma gondii*. Methods Cell Biol. *45*, 28–61.

Russell, D.G., and Sinden, R.E. (1981). The role of the cytoskeleton in the motility of coccidian sporozoites. J. Cell Sci. *50*, 345–359.

Shaw, M.K., and Tilney, L.G. (1999). Induction of an acrosomal process in *Toxoplasma gondii*: visualization of actin filaments in a protozoan parasite. Proc. Natl. Acad. Sci. USA *96*, 9095–9099.

Sibley, L.D., Håkansson, S., and Carruthers, V.B. (1998). Gliding motility: an efficient mechanism for cell penetration. Curr. Biol. *8*, R12–R14.

Stewart, M.J., and Vanderberg, J.P. (1988). Malaria sporozoites leave behind gliding trails of circumsporozoite protein during gliding motility. J. Protozool. *35*, 389–393.

Striepen, B., He, C.Y., Matrajt, M., Soldati, D., and Roos, D.S. (1998). Expression, selection, and organellar targeting of the green fluorescent protein in *Toxoplasma gondii*. Mol. Biochem. Parasitol. *92*, 325–338.

Wu, S.S., and Kaiser, D. (1995). Genetic and functional evidence that type IV pili are required for social gliding motility in *Myxococcus xanthus*. Mol. Microbiol. *18*, 547–558.